

# TEAM: a parameter-free algorithm to teach collaborative robots motions from user demonstrations.

Lorenzo Panchetti,<sup>1</sup> Jianhao Zheng,<sup>1</sup> Mohamed Bouri,<sup>2</sup> and Malcolm Mielle<sup>3</sup>

**Abstract**—Collaborative robots (cobots) built to work alongside humans must be able to quickly learn new skills and adapt to new task configurations. Learning from demonstration (LfD) enables cobots to learn and adapt motions to different use conditions. However, state-of-the-art LfD methods require manually tuning intrinsic parameters and have rarely been used in industrial contexts without experts.

In this paper, the development and implementation of a LfD framework for industrial applications with naive users is presented. We propose a parameter-free method based on probabilistic movement primitives, where all the parameters are pre-determined using Jensen-Shannon divergence and Bayesian optimization; thus, users do not have to perform manual parameter tuning. This method learns motions from a small dataset of user demonstrations, and generalizes the motion to various scenarios and conditions.

We evaluate the method extensively in two field tests: one where the cobot works on elevator door maintenance, and one where three Schindler workers teach the cobot tasks useful for their workflow. Errors between the cobot end-effector and target positions range from 0 to  $1.48 \pm 0.35$  mm. For all tests, no task failures were reported. Questionnaires completed by the Schindler workers highlighted the method’s ease of use, feeling of safety, and the accuracy of the reproduced motion.

Our code and recorded trajectories are made available online for reproduction.

## I. INTRODUCTION

Collaborative robots (cobots) are built to improve society’s welfare by helping people without replacing them. To become an integrated part of our work, cobots must be adaptable and quick-learners: human workers must be able to teach cobots new tasks in a short time, making the robot a new tool in their toolbox. However, it is difficult to transfer skills between a human worker and a cobot—programming the cobot is most of the time done by human experts and cobots cannot adapt to new task configurations, instead repeating learned patterns.

Learning from demonstration (LfD) [1]—a branch of learning focused on skill transfer and generalization through a set of demonstrations—enables cobots to learn and adapt motions from a set of motion demonstrations. For example, when learning how to drill, one only needs to show how to place the part to drill at a specific location and how the drilling

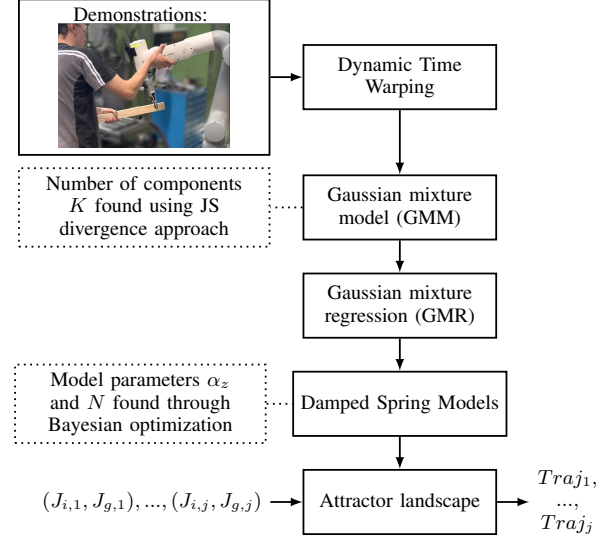


Fig. 1. Flowchart detailing the method of TEAM. A set of demonstrations is recorded by a user and the motion is generalized through GMR. Then, the system is modelled as a set of damped spring models able to generalize the motion to different start and end joint angles. All parameters of the system are automatically optimized and no expert knowledge is needed.

machine works. Moving the object and/or the drill position is not a problem for a human since we can generalize skills to various task spaces and objectives. However, state-of-the-art LfD methods require manually tuning intrinsic parameters and have thus rarely been used in industrial contexts without experts. In this paper, we present TEAM (teach a robot arm to move), a novel method to learn from demonstrations without parameters tuning.

The main contributions of this paper are:

- Development of TEAM, a parameter-free framework to learn motions from a set of demonstrations. This method uses a generative model to find a generalized trajectory and builds attractor landscapes to reproduce the motion between different start and end joint angles.
- An optimization strategy of the attractor landscape’s intrinsic parameters through Bayesian optimization.
- Improvement on the selection of the number of Gaussian Mixture Models through Jensen-Shannon divergence.
- Implementation and experimental validation of TEAM in two field tests showing that our method can be used by naive users.

The overview of the methodology is shown in Fig. 1.

## II. RELATED WORK

Rana et al. [1] present a large-scale study benchmarking the performance of motion-based LfD approaches. They train 180

This work was supported by Schindler AG

<sup>1</sup>Lorenzo Panchetti and Jianhao Zheng are Master students at the école polytechnique fédérale de Lausanne (EPFL), 1015 Lausanne, lorenzo.loredano.panchetti@gmail.com jianhaozheng1@gmail.com

<sup>2</sup>Mohamed Bouri is the group leader of the REHAssist group at the école polytechnique fédérale de Lausanne (EPFL), 1015 Lausanne, mohamed.bouri@epfl.com

<sup>3</sup>Malcolm Mielle is the head of the REGiS lab of Schindler AG at the école polytechnique fédérale de Lausanne, 1015 Lausanne malcolm.mielle@schindler.com

task models and evaluate 720 task reproductions on a physical robot. Probabilistic movement primitive (ProMP) methods are shown to be the most consistent on tasks with positional constraints which is why TEAM is based on ProMP.

To model a set of demonstrations, Ahmadzadeh et al. [2] use a geometric model composed of a regular curve and a canal surface [3]. Their method doesn't require parameter tuning, maintains the main characteristics and implicit boundaries of the trajectory, but cannot adapt to goal positions outside the canal surface.

Calinon et al. [4] fit a mixture of Gaussian on a set of demonstrations and generalizes the motion through Gaussian Mixture Regression (GMR) [5]. Trajectories are computed by optimizing an imitation performance metric, enabling the robot to generalize a learned task to contexts not seen in the demonstration set. However, joint configurations are not constrained to the demonstration space, which can lead to the exploration of unsafe areas.

Schaal [6] and Ijspeert et al. [7] use Dynamical Movement Primitives (DMP) to model complex motions through nonlinear dynamical systems. DMP is scale and temporal invariant, convergence is proven, but the parameters of the system must be manually tuned.

Pervez et al. [8] propose a method that generalizes motion outside the demonstrated task space. Each demonstration is associated with a dynamical system, and learning is formulated as a density estimation problem. However, parameters must be set empirically for all dynamical systems—a time-consuming task incompatible with use by naive users.

Recent works have leveraged advances in deep learning. Pahič et al. [9] propose to train a neural network to output the parameters of the DMP model from an image, before learning the associated forcing term. Pervez et al. [10] use deep neural networks to learn the forcing terms of the DMP model for vision-based robot control. Both methods involve a convolutional neural network learning task-specific features from camera images. Sanni et al. [11] estimate the correlation between visual information and ProMP weights for reach-to-palpat motion. The average error in task space is around 3 to 5 centimeters which is too high for our application. Yang et al. [12] use reinforcement learning to learn a latent action space representing the skill embedding from demonstrated trajectories for each prior task. All methods based on deep or reinforcement learning require a large amount of data. E.g., Sanni et al. [11] show the robot the reach-to-palpat motion 500 times, Pervez et al. [10] acquire 50 demonstrations for a single task, and Yang et al. [12] uses around 80K trajectories.

### III. METHOD

TEAM builds on previous work on ProMP [4] and attractor landscape [7]. First, a set of demonstrations for a given task is collected by the user. A demonstration stores the cobot's joints angles recorded while the cobot is shown the task in gravity compensation mode—see the image in the demonstration box of Fig. 1. The robot is controlled in joint space to be able to use redundant robot arms, and to avoid singularities during the motion. All demonstrations are aligned in time

using dynamic time warping [13]. Section III-A shows how the Jensen-Shannon (JS) divergence [14] can be used to find the best Gaussian mixture model (GMM) fit on the demonstrations dataset and calculates the Gaussian Mixture Regression (GMR)—i.e. the generalized trajectory. Section III-C shows how the optimal damped spring model parameters are estimated through Bayes optimization. Finally, Section III-D presents how the optimal motion is computed by the attractor landscape, given the initial and goal cobot joints angles.

#### A. Gaussian Mixture Model and Gaussian Mixture Regression

Given a set of demonstrations, the first step of the method is to fit a GMM on all degrees of freedom—each of the cobot's joints. Maximum Likelihood Estimation of the mixture parameters is performed iteratively using Expectation Maximization (EM) [15].

The number of mixture model components  $K$  is critical to obtaining a GMM leading to a smooth GMR. Calinon et al. [4] use the BIC criterion to determine the optimal value  $K$ , but, as shown by Pervez et al. [10], BIC overfits the dataset without a regularization factor—our dataset can be small and BIC is only valid for sample size much larger than the number of parameters in the model [16]. Pervez et al. [8] on the other hand use deterministic annealing expectation maximization [17] which depends on a parameter for the temperature schedule. While  $K$  needs to be updated every time a new demonstration is added to the demonstration dataset, selecting the optimal value of  $K$  has previously been dependent on manual thresholds—and thus, time-consuming.

The best GMM fit is hypothesized to be consistent over multiple fitting with a constant value of  $K$ : sub-optimal values of  $K$  lead to non-repeatable fits due to under- or over-fitting of the Gaussian distributions. Hence, to improve the selection of the optimal number of components, the similarity between two probability distributions is calculated with the JS divergence. The process to estimate the JS divergence for  $K = 2$  until  $K = m$ , with  $m$  the maximum number of components in the GMM, is shown in Algorithm 1 from Line 1 to Line 10. First, the datapoints in the dataset of demonstrations are randomly and evenly split into training and testing sets. Then, a GMM with  $K$  components is fitted on each set separately using EM and the JS divergence between training and testing mixtures is calculated. Since EM only guarantees that the GMM fit converges to a local optimum, we run this process 50 times per  $K$  and calculate the standard deviation and mean.

The optimal value of  $K$  is determined through a series of one-tailed Welch's t-test [18]. We select  $l$  to be the number of components with the lowest mean JS divergence and calculate the p-value between  $l$  and all other components. The null hypothesis is that the mean JS divergence of  $l$  isn't smaller than all the other values of  $K$ . We choose  $\alpha = 0.05$ —meaning that there is a 5% chance that the results occurred at random. If the p-value  $p_{lk}$  between the distributions for  $l$  and  $k$  components is smaller than  $\alpha$ , the null hypothesis is rejected. On the other hand, if  $p_{lk}$  is larger than  $\alpha$ , the test does not reject the null hypothesis.

**Data:** demonstrations set  $D$

**Result:**  $best_K$

```

1  $C \leftarrow$  empty map;
2 for  $K = 2$  until  $K = m$  do
3    $res \leftarrow$  empty list;
4   for  $l$  to 50 do
5     Sample datapoints of demonstrations of  $D$  in
       two sets;
6     Fit a GMM with  $n$  components on each set;
7     Add JS divergence to  $res$ ;
8   end
9    $C(n) \leftarrow res$ ;
10 end
11  $l \leftarrow$  component in  $C$  with the lowest mean;
12  $best_K \leftarrow l$ ;
13 for key  $m$ , value  $v \in C$  do
14   if  $p_{lm} > 0.05$  and  $std$  of  $v < std$  of  $C(best_K)$ 
       then
15      $best_K \leftarrow m$ ;
16   end
17 end
18 return  $best_K$ 

```

**Algorithm 1:** Algorithm used to determine the best number of components for the Gaussian Mixture Model.

Given  $s$  the set containing  $l$  and every value of  $K$  that does not reject the null hypothesis, the optimal number of components is the element in  $s$  with the lowest standard deviation—i.e. the number of components with the most stable fit. The process to determine the optimal number of Gaussians is detailed in Algorithm 1 from Line 11 to Line 18.

### B. Damped spring model

TEAM uses the damped spring model formulated by Ijspeert et al. [7]. In this paper, a summary of the seminal formulation and the method's contributions are presented.

The system is represented as a damped spring model:

$$\begin{aligned} \tau \dot{z} &= \alpha_z (\beta_z (g - y) - z) + f \\ \dot{y} &= z \end{aligned} \quad (1)$$

where  $\tau$  is a time constant,  $f$  is the nonlinear forcing term, and  $\alpha_z$  and  $\beta_z$  are positive constants. The forcing term  $f$  of Eq. (1) is used to produce a specific trajectory—i.e. the GMR. Since  $f$  is a nonlinear function, it can be represented as a normalized linear combination of basis functions [19]:

$$f(x) = \frac{\sum_{i=1}^N \Psi_i(x) \omega_i}{\sum_{i=1}^N \Psi_i(x)} (g - y_0) v \quad (2)$$

where  $\Psi_i$  are fixed radial basis functions,  $\omega_i$  are the weights learned during the fit,  $g$  is the goal joint angles, and  $v$  is the system velocity.  $N$  is the number of fixed radial basis function kernels  $\Psi_i(x)$ :

$$\Psi_i(x) = \exp\left(-\frac{1}{2\sigma_i^2}(x - c_i)^2\right) \quad (3)$$

where  $\sigma_i$  and  $c_i$  are values that determine, respectively, the width and centers of the basis functions and  $y_0$  is the initial state  $y(t=0)$ . Details of the derivation of the forcing term

are found in Ijspeert et al. [7]. A spring model is estimated for each degree of freedom and a shared canonical system [7] synchronize them in time.

### C. Parameters optimization

For  $y$  to monotonically converge towards the target  $g$ , the system must be critically damped on the GMR by choosing the appropriate values of  $\alpha_z$  and  $\beta_z$ . As shown by Ijspeert et al. [7],  $\beta_z$  can be expressed with respect to  $\alpha_z$  as  $4\beta_z = \alpha_z$ . Thus, only two parameters control the tracking of the reference and the stability: the number of radial basis functions  $N$  and the constant  $\alpha_z$ . In the previous work of Ijspeert et al. [7] and Pervez et al. [8],  $\alpha_z$  and  $N$  are empirically chosen by the user. As far as we know, this work is the first attempt to present a method to determine those parameters without relying on manual tuning.

$\alpha_z$  and  $N$  are found through Bayesian optimization (BO) [20]. The error to minimize is the sum of both the root mean squared error with respect to the GMR and the distance of the trajectory endpoint with respect to the goal reference:

$$f(\alpha_z, N) = \sqrt{\frac{\sum_{t=1}^T (y(\alpha_z, N, t) - y_G(t))^2}{T}} + \|y(\alpha_z, N, T) - y_G(T)\| \quad (4)$$

where  $y(\alpha_z, N, t)$  is the joints angle at time  $t$  obtained with DMP parameters  $\alpha_z$  and  $N$ ,  $y_G(t)$  is the GMR joints angle at time  $t$ , and  $\|\cdot\|$  is the  $l_2$ -norm. The acquisition function is the expected improvement (EI):

$$EI_i(x) := E_i[f(x) - f_i^*] \quad (5)$$

where  $E_i[\cdot|x_{1:i}]$  indicates the expectation taken under the posterior distribution given evaluations of  $f(x)$  at  $x = x_1, \dots, x_i$ . The acquisition function retrieves the point in the search space that corresponds to the largest expected improvement and uses it for the next evaluation of the objective function  $f(x)$ . The point  $x_i$  minimizing the value of  $f(x)$  corresponds to the optimal combination of  $\alpha_z$  and  $N$ . The optimization is stopped when two successive query points are equal: upon reaching the function's minimum, EI returns the same query point since no other points can improve the estimation of the minimum.

A study of the repeatability of the optimization method is provided in Section IV-B.

### D. Parameters $\omega_i$ and joint dynamic

We compute the parameters  $\omega_i$  as per the method of Ijspeert et al. [7]. Here a short explanation of those calculations is given, but more details can be found in the original paper.

The parameters  $\omega_i$  are learned using locally weighted regression (LWR) [21]. When inserting the joints angle, velocity, and acceleration information, Eq. (1) becomes:

$$f_{target} = \tau^2 \ddot{y}_{demo} - \alpha_z (\beta_z (g - y_{demo}) - \tau \dot{y}_{demo}) \quad (6)$$

LWR finds for each kernel function  $\Psi_i$  in  $f$  the corresponding  $\omega_i$ , which minimizes the locally weighted quadratic

error criterion:

$$J_i = \sum_{t=1}^P \Psi_i(t) (f_{target}(t) - \omega_i \lambda(t))^2 \quad (7)$$

where  $\lambda(t) = x(t)(g - y_0)$  for the discrete system. This is a weighted linear regression problem, which has the solution:

$$\omega_i = \frac{s^T \Gamma_i f_{target}}{s^T \Gamma_i s} \quad (8)$$

Given  $I_d$  the identity matrix:

$$s = \begin{pmatrix} \lambda(1) \\ \vdots \\ \lambda(P) \end{pmatrix} \quad \Gamma_i = \begin{pmatrix} \Psi_i(1) \\ \vdots \\ \Psi_i(P) \end{pmatrix} * I_d \quad (9)$$

Finally, the forcing term is learned by plugging equations Eq. (8) and Eq. (3) into equation Eq. (2).

With initial conditions  $(y_0, 0, 0)$ , the joint dynamics evolution  $(y_d, \dot{y}_d, \ddot{y}_d)$  can be computed iteratively by integration. At each time step, the weighted sum of the locally weighted models and the current forcing term for each DOF  $d$  are calculated. The dynamical systems equations are solved according to the following scheme:

$$\begin{aligned} \dot{v}_i &= \alpha_v(-\beta_v x_i - v_i)\tau & \dot{x}_i &= v_i\tau \\ \dot{z}_i &= (\alpha_z(\beta_z(g_i - y_i) - z_i) + f_i)\tau \\ \dot{y}_i &= z_i\tau & \dot{y}_i &= \dot{z}_i\tau \\ \dot{g}_i &= \alpha_g(G_i - g_i) & x_i &= \dot{x}_i\Delta t + x_i \\ v_i &= \dot{v}_i\Delta t + v_i & z_i &= \dot{z}_i\Delta t + z_i \\ y_i &= \dot{y}_i\Delta t + y_i & g_i &= \dot{g}_i\Delta t + g_i \end{aligned}$$

where  $\Delta t$  is equal to the data acquisition interval of 0.01s.

#### IV. EVALUATION

We evaluate our method in two real-world scenarios: one where the cobot works alone to do maintenance operations on an elevator door, and one where workers teach the cobot tasks needed in a drilling scenario. Public implementation can be found online.<sup>1</sup> A 6 axis ABB GoFa CRB 15000 cobot is used.<sup>2</sup> Pose repeatability at the maximum reach and load is 0.05 mm, and axis resolution is  $1.74 \cdot 10^{-5}$  rad.

In our scenarios, it is important that the cobot accurately reaches the target joint position. Given  $g$  the goal joint position and  $c$  the actual end joint position, we measure:  $e_j$  the joints distance between  $g$  and  $c$ ,  $e_p$  the  $l_2$  norm between the endpoint position and the target goal, and  $e_\theta$  the orientation error between  $g$  and  $c$ :

$$\begin{aligned} H_r &= (H_c)^{-1} H_g \\ e_\theta &= \|H_r - I\| \end{aligned} \quad (10)$$

with  $H_c$  and  $H_g$  the homogeneous rotation matrices describing  $c$  and  $g$  orientations, and  $I$  the identity matrix.

Rana et al. [1] show that the mean squared error (MSE) of the trajectory compared to the reference trajectory is not a

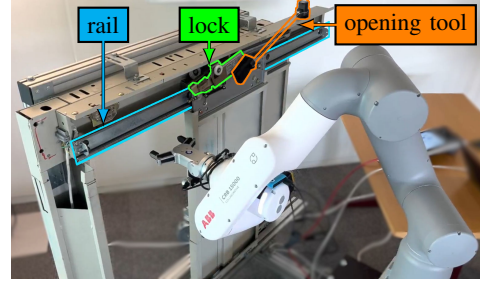


Fig. 2. The ABB GoFa cobot is facing the test elevator door used for evaluation of TEAM in a maintenance scenario.

good metric of trajectory reproduction since it measures deviations from the set of demonstrations instead of adaptability. Since MSE penalizes the distance from a reference signal, MSE would assign a lower score to a successful trajectory adapting to different starting and end conditions, than to a trajectory close to the regression. In our work, we visually evaluate the reproductions and consider a reproduction failed if 1) the movement does not look like the demonstration, 2) the cobot collides with any element of the environment, 3) the task fails—e.g. the tool does not keep the door open or the brush is not in its support.

##### A. Elevator door maintenance

Elevator door maintenance consists of 5 tasks:

- T1: open and lock the door using a custom opening tool. The lock is now in the middle of the rail.
- T2: grab the cleaning tool.
- T3: clean the rail while avoiding the lock. The cobot must aim for both ends of the rail with the brush since most dust accumulates there.
- T4: drop the cleaning tool on its support.
- T5: grab the opening tool, close the door, and combine the two pieces of the opening tool.

The maintenance setup can be seen in Fig. 2. Opening and locking the door is done using a custom tool grabbed by the cobot. To open the door the cobot must follow a complex motion of rotations and translations. The position of the cleaning tool before cleaning is known at all times since it is on a fixed support next to the cobot. However, the position of the door is changed between each evaluation run, ensuring that no trajectory will be the same. We detect specific elements of the door using a custom-trained neural network based on YOLACT++ [22] and extrapolate all start and target positions from those door elements.

Table I shows the number of demonstrations with the training and trajectory reproduction times of each task. The maximum training time is under 4min—the longest training time is  $203.33 \pm 4.32$ s for T2. The complexity of DTW is  $\mathcal{O}((M-1)L^2)$ , with  $M$  being the number of demonstrations in the dataset and  $L$  the longest demonstration length, GMM and GMR with full covariance matrices are  $\mathcal{O}(KBD^3)$  where  $B$  is the number of datapoints in the dataset,  $D$  the data dimensionality, and  $K$  the number of GMM components. Finally, the Gaussian Process of the BO is  $\mathcal{O}(R^3)$  with  $R$  being the number of function evaluations—Table III shows

<sup>1</sup><https://github.com/SchindlerReGIS/team>

<sup>2</sup><https://new.abb.com/products/robotics/collaborative-robots/crb-15000>

TABLE I

THIS TABLE PRESENTS THE TRAINING TIME AND ERROR METRICS FOR THE MAINTENANCE TASK— 10 RUNS ARE PERFORMED PER TASK. FAILURES CORRESPOND TO THE NUMBER OF TIME THE ROBOT FAILED EITHER BY NOT REPRODUCING THE MOVEMENT OR BY NOT COMPLETING THE TASK.

Task	T1	T2	T3	T4	T5
Name	Open the door	Pick up brush	Clean rail	Deposit brush	Close the door
Nb demonstrations	6	4	4	4	3
Average demonstration duration [s]	33.19 $\pm$ 2.38	36.37 $\pm$ 2.28	32.93 $\pm$ 3.00	28.17 $\pm$ 3.33	26.19 $\pm$ 1.05
DTW [s]	104.41 $\pm$ 0.64	104.35 $\pm$ 1.61	93.27 $\pm$ 0.53	67.75 $\pm$ 2.92	56.57 $\pm$ 1.57
GMM + GMR [s]	64.54 $\pm$ 1.16	77.82 $\pm$ 3.29	79.68 $\pm$ 0.53	75.27 $\pm$ 2.86	78.11 $\pm$ 2.39
BO [s]	14.69 $\pm$ 1.57	20.78 $\pm$ 1.91	12.46 $\pm$ 2.82	19.55 $\pm$ 2.21	13.55 $\pm$ 2.53
ProMP[s]	0.44 $\pm$ 0.01	0.39 $\pm$ 0.01	0.41 $\pm$ 0.01	0.31 $\pm$ 0.02	0.35 $\pm$ 0.04
Total time [s]	184.08 $\pm$ 2.45	203.33 $\pm$ 4.32	185.82 $\pm$ 3.07	162.89 $\pm$ 4.56	148.59 $\pm$ 4.51
Position error $e_p$ [mm]	1.06 $\pm$ 0.28	0.89 $\pm$ 0.01	1.48 $\pm$ 0.35	0 $\pm$ 0	0.73 $\pm$ 0.01
Orientation error $e_\theta$	0.002 $\pm$ 0.001	0.004 $\pm$ 0.001	0.005 $\pm$ 0.002	0.001 $\pm$ 10 <sup>-5</sup>	0.002 $\pm$ 10 <sup>-5</sup>
Joints error $e_j$ [rad]	0.013 $\pm$ 0.006	0.008 $\pm$ 0.003	0.007 $\pm$ 0.002	0.008 $\pm$ 0.002	0.007 $\pm$ 0.002
Failures	0	0	0	0	0

TABLE II

THE TABLE SHOWS THE JENSEN-SHANNON DIVERGENCE REPEATABILITY OVER 50 DIFFERENT RUNS. THE NUMBER OF GMM COMPONENTS RANGES FROM 2 TO 9.

Task	T1	T2	T3	T4	T5
Median nb GMM	5 $\pm$ 0.40	3 $\pm$ 0	4 $\pm$ 0	3 $\pm$ 0	4 $\pm$ 0.27

that  $R$  is at worse around  $34.20 \pm 10.85$ . Hence, training time depends on the number of demonstrations and their lengths. It should be noted that training happens only once and the cobot does not need to be retrained to perform the trajectory for different task configurations.

The cobot never failed a motion, and errors in position are small, showing that the cobot accurately reaches the target joint position.  $T1$  and  $T3$  have slightly higher errors due to interaction with the environment. In  $T1$ , the door's spring applies a force on the robot during the movement but is released when the tool locks the door. The pressure release slightly moves the cobot out of its target position. In  $T3$ , the friction of the sponge on the rail acts similarly.

### B. Evaluation of the parameters' repeatability

A repeatability analysis of the parameters  $K$ ,  $\alpha_z$ , and  $N$ , is done on the data collected for the door maintenance scenario.

*Repeatability of  $K$  using the JS divergence:* the method described in Section III-A is ran 50 times for each demonstrations dataset of the maintenance scenario. As seen in Table II, the median number of Gaussians for each dataset is either fixed, or varies only by a small standard deviation.

*Damped spring model parameters:* as seen in Table III, BO converges to the global optimum of the function—BO minimum values are the same as a grid search over the entire search space. Optimization took an average of 19.57s on an Intel Core i5 10<sup>th</sup> Gen. Different optimization times are due to the random initial sampling and the prior distribution built on the surrogate function at the beginning of each run. The convergence time of the BO process is between 5% and 20% of the overall model training time for all tasks. In Fig. 3, one can see that larger standard deviation in the running time are usually due to larger outliers. For the same 2D search space,

TABLE III

COMPARISON BETWEEN GRID SEARCH (GS) AND BAYESIAN OPTIMIZATION (BO). STATISTICS ARE COMPUTED OVER 50 RUNS.

Task	T1	T2	T3	T4	T5
GS minimum	12.84	73.91	30.88	36.58	26.44
BO minimum	12.84 $\pm 0$	74.22 $\pm 0.61$	30.98 $\pm 0.40$	36.68 $\pm 0.27$	26.44 $\pm 0.05$
GS time [s]	2348.97	2600.96	2427.34	2149.50	1848.20
BO median time [s]	19.39 $\pm 3.63$	27.40 $\pm 10.17$	12.40 $\pm 2.40$	26.11 $\pm 18.54$	12.53 $\pm 1.99$
GS calls	3750	3750	3750	3750	3750
BO calls	23.14 $\pm 3.88$	34.20 $\pm 10.85$	16.96 $\pm 2.73$	32.98 $\pm 18.97$	20.14 $\pm 2.58$

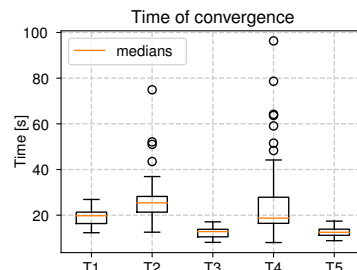


Fig. 3. Bayesian optimization times for each task over 50 runs.

grid search is between a factor of 50 to 100 slower than BO due to the larger number of evaluations computed.

### C. Field tests

We conducted field tests at the Schindler headquarters in Ebikon. To be realistic, the scenarios were designed with field workers. With the support of an expert roboticist, they created four scenarios that were relevant to their work, and would help reducing their workload if the robot could easily be taught how to perform the task:

- $F1$ : find a metal piece (see Fig. 4a), grab it, and place it accurately on a drilling machine.
- $F2$ : find a metal piece, grab it, and place it accurately on a drilling machine while avoiding an obstacle.
- $F3$ : find a metal frame (see Fig. 4b), grab it, and place it accurately on a drilling machine while rotating the piece.



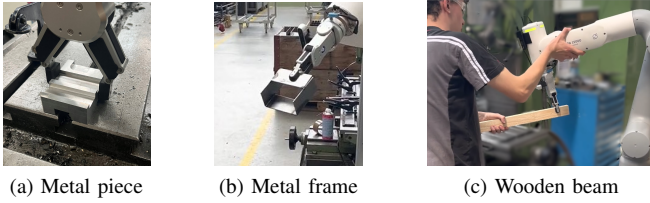


Fig. 4. Objects used during field tests.



Fig. 5. For the factory field tests, the robot was placed in the training section of the Schindler offices with a drilling machine (in green in the image). Users were tasked to teach the robot specific motions that could be used in their work. The focus was on pick and place for drilling. The three objects used are shown in Fig. 4.

- *F4*: find a wooden plank (see Fig. 4c), grab one side while the worker grabs the other, and, place it together accurately on a drilling machine.

The testing setup can be seen in Fig. 5 and detection of the different objects is done with template matching.

The tests were conducted by three Schindler workers, and for each task, three to five demonstrations per user were collected. Results presented in Table IV were calculated for 30 reproductions of the motion for each task.

#### D. User survey

At the end of each day, the workers could answer a questionnaire to evaluate the cobot's performance. In the survey, users rate the following statements on a scale from 1 to 5, corresponding to strongly disagree, disagree, neutral, agree, and strongly agree:

- The cobot learned the correct motion.
- I felt safe operating the cobot.
- The cobot reached the goal point accurately.
- Teaching the cobot a motion was simple.
- Teaching the cobot a motion was entertaining.

The radar plots in Fig. 6 present the survey's results. While users show satisfaction with the cobot's precision and motion performance, the complexity of holding the beam and moving the cobot while demonstrating the motion in *F4* lead to lower score for easiness of teaching compared to other tasks.

#### V. LIMITATIONS AND FUTURE WORK

TEAM doesn't take into account elements of the environment during the motion. This can create confusion for the workers not understanding why the cobot does not avoid

TABLE IV

THIS TABLE PRESENTS ERROR METRICS FOR THE FACTORY SCENARIO—30 RUNS ARE PERFORMED PER TASK.

Task	F1	F2	F3	F4
Name	Drill	Avoid	Parallel	Collaborative
Position error $e_p$ [mm]	$0 \pm 0$	$0.15 \pm 0.03$	$0.54 \pm 0.65$	$0.29 \pm 0.29$
Orientation error $e_\theta$	$5.2 \cdot 10^{-5} \pm 3.4 \cdot 10^{-5}$	$9.6 \cdot 10^{-4} \pm 7.2 \cdot 10^{-4}$	$4.7 \cdot 10^{-4} \pm 5.5 \cdot 10^{-4}$	$0.001 \pm 0.001$
Joints error $e_j$ [rad]	$0.618 \pm 0.517$	$0.580 \pm 0.274$	$0.573 \pm 0.228$	$0.594 \pm 0.199$
Failures	0	0	0	0

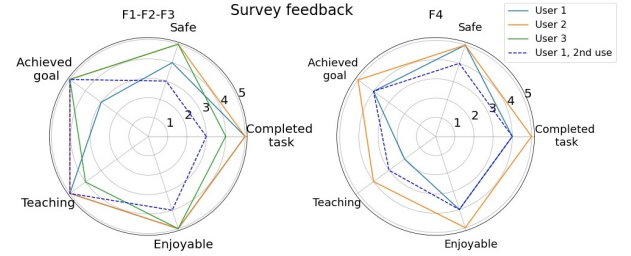


Fig. 6. The cobot interaction is evaluated in terms of safety, easiness to teach, entertainment, goal achievement, and task completion. Three answers have been collected for results in the chart on the right, featuring two different users. A user participated in the activities twice, its second feedback is shown in dashed lines.

obstacles, making it harder for them to trust the cobot. Future work will look at integrating visual information through cameras to update the motion depending on the environment.

Another way that TEAM could be improved is by being able to update the attractor landscape of a motion incrementally. Currently, if a new demonstration is added to an existing motion dataset, the cobot needs to run the full training procedure. Future work will look into making the process incremental, giving workers the ability to correct existing motions learned by the cobot, instead of re-training the model from scratch.

#### VI. SUMMARY

A method to learn motions from demonstrations requiring no manual parameter tuning has been developed. Given a set of demonstrations aligned in time, the motion is generalized using GMM and the reference trajectory is extracted with GMR. Since BIC criterion can lead to overfitting of the GMM, it's proposed to instead use the Jensen-Shannon divergence to determine the optimal number of GMM components. The cobot DOFs are represented as damped spring models and the forcing term is learned to adapt the motion to different start and goal joint poses. Parameters of the spring model are found using Bayesian optimization.

TEAM is extensively evaluated in two field tests where the cobot performs tasks related to elevator door maintenance, and works with workers directly in the field. The evaluation shows that the cobot is positively accepted by the workers since it is easy to teach, easy to use, and safe. Furthermore, both the precision in position and the failure rate of the cobot are measured—experiments show that the cobot reproduces the motions with a maximum error in position of  $1.48 \pm 0.35$ mm, and a failure rate of 0%.

# REFERENCES

- [1] M. A. Rana, D. Chen, S. R. Ahmadzadeh, J. Williams, V. Chu, and S. Chernova, "Benchmark for skill learning from demonstration: Impact of user experience, task complexity, and start configuration on performance," *2020 IEEE International Conference on Robotics and Automation (ICRA)*, pp. 7561–7567, 2020.
- [2] S. R. Ahmadzadeh and S. Chernova, "Trajectory-based skill learning using generalized cylinders," *Frontiers in Artificial Intelligence and Applications*, vol. 5, p. 132, Dec. 2018. DOI: 10.3389/frobt.2018.00132.
- [3] D. Hilbert and S. Cohn-Vossen, "Geometry and the imagination," *Chelsea Publishing Company, New York*, 1952.
- [4] S. Calinon, F. Guenter, and A. Billard, "On learning, representing, and generalizing a task in a humanoid robot," *IEEE Transactions on Systems, Man, and Cybernetics, Part B (Cybernetics)*, vol. 37, pp. 286–298, 2007.
- [5] D. A. Cohn, Z. Ghahramani, and M. I. Jordan, "Active learning with statistical models," in *NIPS*, 1996.
- [6] S. Schaal, "Dynamic movement primitives -a framework for motor control in humans and humanoid robotics," in *Adaptive Motion of Animals and Machines*, H. Kimura, K. Tsuchiya, A. Ishiguro, and H. Witte, Eds. Tokyo: Springer Tokyo, 2006, pp. 261–280, ISBN: 978-4-431-31381-6. DOI: 10.1007/4-431-31381-8\_23.
- [7] A. J. Ijspeert, J. Nakanishi, H. Hoffmann, P. Pastor, and S. Schaal, "Dynamical Movement Primitives: Learning Attractor Models for Motor Behaviors," *Neural Computation*, vol. 25, no. 2, pp. 328–373, Feb. 2013, ISSN: 0899-7667. DOI: 10.1162/NECO\_a\_00393.
- [8] A. Pervez and D. Lee, "Learning task-parameterized dynamic movement primitives using mixture of gmms," *Intelligent Service Robotics*, vol. 11, pp. 61–78, 2018.
- [9] R. Pahič, B. Ridge, A. Gams, J. Morimoto, and A. Ude, "Training of deep neural networks for the generation of dynamic movement primitives," *Neural networks : the official journal of the International Neural Network Society*, vol. 127, pp. 121–131, 2020.
- [10] A. Pervez, Y. Mao, and D. Lee, "Learning deep movement primitives using convolutional neural networks," *2017 IEEE-RAS 17th International Conference on Humanoid Robotics (Humanoids)*, pp. 191–197, 2017.
- [11] O. Sanni, G. Bonvicini, M. A. Khan, P. C. López-Custodio, K. Nazari, and E. AmirM.Ghahamzan, "Deep movement primitives: Toward breast cancer examination robot," *ArXiv*, vol. abs/2202.09265, 2022.
- [12] Q. Yang, J. A. Stork, and T. Stoyanov, "Mpr-rl: Multi-prior regularized reinforcement learning for knowledge transfer," *IEEE Robotics and Automation Letters*, pp. 1–8, 2022. DOI: 10.1109/LRA.2022.3184805.
- [13] H. Sakoe and S. Chiba, "Dynamic programming algorithm optimization for spoken word recognition," *IEEE Transactions on Acoustics, Speech, and Signal Processing*, vol. 26, pp. 159–165, 1978.
- [14] J. Lin, "Divergence measures based on the shannon entropy," *IEEE Transactions on Information Theory*, vol. 37, no. 1, pp. 145–151, 1991. DOI: 10.1109/18.61115.
- [15] A. P. Dempster, N. M. Laird, and D. B. Rubin, "Maximum likelihood from incomplete data via the em algorithm," *Journal of the Royal Statistical Society: Series B (Methodological)*, vol. 39, no. 1, pp. 1–22, 1977. DOI: <https://doi.org/10.1111/j.2517-6161.1977.tb01600.x>.
- [16] C. Giraud, "Introduction to high-dimensional statistics," 2014. DOI: <https://doi.org/10.1201/b17895>.
- [17] N. Ueda and R. Nakano, "Deterministic annealing em algorithm," *Neural networks : the official journal of the International Neural Network Society*, vol. 11 2, pp. 271–82, 1998.
- [18] W. Bl, "The generalization of 'student's' problem when several different population variances are involved," *Biometrika*, vol. 34, pp. 28–35, 1947.
- [19] C. M. Bishop, "Pattern recognition and machine learning (information science and statistics)," 2006.
- [20] R. Garnett, *Bayesian Optimization*. Cambridge University Press, 2022, in preparation.
- [21] S. Schaal and C. G. Atkeson, "Constructive incremental learning from only local information," *Neural Computation*, vol. 10, pp. 2047–2084, 1998.
- [22] D. Bolya, C. Zhou, F. Xiao, and Y. J. Lee, "Yolact++ better real-time instance segmentation," *IEEE Transactions on Pattern Analysis and Machine Intelligence*, vol. 44, pp. 1108–1121, 2022.